WIDMANSTÄTEN PATTERN RESPONSE TO IMPACTS. R. J. Lyons[1], F. J. Ciesla[1], and N. Dauphas[1,2], [1]The Department of the Geophysical Sciences, The University of Chicago, Chicago, Illinois (rjlyons@uchicago.edu), [2]Origins Laboratory and Enrico Fermi Institute, The University of Chicago, Chicago, Illinois.

Introduction: Iron meteorites come from the cores of differentiated planetesimals. The Widmanstäten pattern found in these samples developed from the exsolution of kamacite (α, body-centered cubic) from taenite (γ, face-centered cubic) as the core cooled. This growth is temperature dependent, allowing the grain sizes and Ni-concentrations to be used to determine the cooling rate that the core experienced. The cooling rates of these samples provide valuable insight into the thermal evolution and structures of their parent bodies. Early models for the thermal evolution of planetesimals predicted that cores would cool uniformly, such that each part of the core cooled at the same rate, and that these cooling rates indicated the sizes of the planetesimal that each meteorite came from [1]. However, several iron meteorite groups exhibit cooling rates that range over orders of magnitude. For example, IVA iron meteorites have measured cooling rates from 100 to 6600 K/Myr [2], which cannot be produced by a single parent body in the framework of these early models.

Impacts that occur when a body is hot can alter the structures of differentiated planetesimals, eroding the insulating mantle above the core in some regions [3]. Depending on the time of the impact, this can accelerate the rate of cooling that a given body will experience while also leading to orders of magnitude variation in cooling rates in a single core. It is not clear, however, how the formation of the Widmanstäten patterns in these disturbed samples would be affected by changes in cooling rate. If the final Ni concentration profile is different than a non-impacted body the cooling rate of a given sample might be misreported. Here we report preliminary results of our investigation of whether changes in cooling caused by energetic collisions in the early Solar System would lead to distinguishing features in the Widmanstäten patterns in iron meteorites.

Diffusion Model: We follow the 1-D Ni diffusion model described in [4]. The model utilizes a front-tracking, fixed finite-difference grid method described by [5]. We assume kamacite nucleates at regular intervals throughout the melt. The model focuses on the half-distance between two kamacite nucleation sites; this distance is known as the impingement length and is denoted by L. These nucleation sites are assumed to repeat infinitely so no-flux boundary conditions are used. For our undisturbed models, the simulation begins at the nucleation temperature of kamacite (~700 C), the cooling rate is held constant, and the material cools to 450 C (below which the diffusion of Ni is negligible). We follow the change in concentration of Ni via diffusion as a function of time using Fick's second law. The concentration at the interface between the kamacite and the taenite is set by the phase diagram [6]. The interface position is also calculated over time as the concentration profile changes. It is allowed to move to the left or the right depending on the differentials of the Ni concentrations on either side of the interface boundary.

To test the model, we apply it to the simplified, though unphysical, diffusion problem outlined by [7], for which an analytic solution is derived. Figure 1 shows the profile and agreement between our model and the analytic solution. We have also worked to ensure that the results of the code are independent of numerical resolution, and thus are confident in our results.

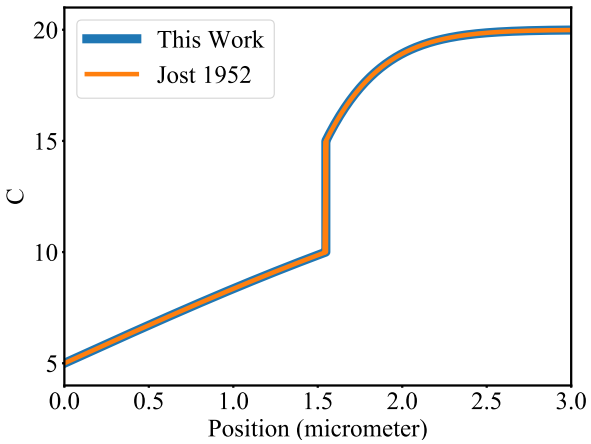

Figure 1: Test of our diffusion model looking at an unphysical situation with an analytical solution determined in Jost 1952. After 1 year of model time our model is nearly identical to the analytic solution.

Preliminary Results: We ran a suite of simulations to determine the final Ni concentration profile in a sample for constant cooling rates between 1 and 10,000 K/Myr. For the runs reported here the impingement length is set to L=700 μm with a bulk Ni content of 8.16 wt%, the same as the reference model for the meteorite Toluca [6]. There is also no phosphorus in these simulations. The presence of P would affect the phase diagram and diffusivity of the materials [4,6]. We will be considering these effects in future work, but use this suite of cases as the base models for our initial investigation. Figure 2 is an example of a few constant cooling rate Ni profiles. The large jumps in concentration represent the transition from kamacite (left side) to taenite (right side). As the iron cools the concentration of Ni due to taenite formation at the interface increases. The position of this interface also moves to the rights as the

kamacite grows. Note the positions of the half-widths and central Ni concentrations of the taenite bands. The slower the cooling rate the narrower the taenite band and the higher the central Ni concentrations.

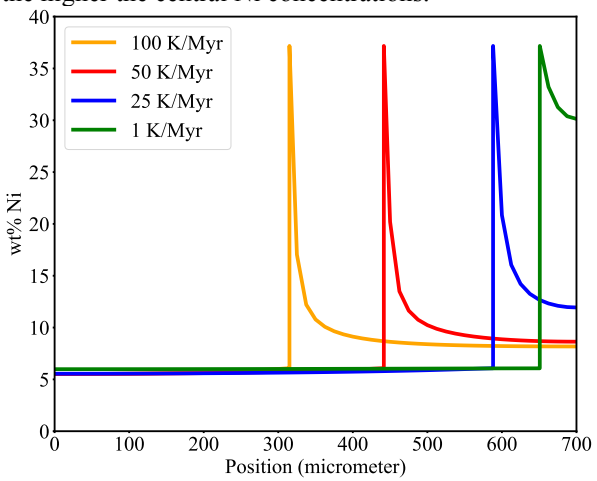

Figure 2: A collection of Ni concentration profiles for constant cooling rates showcasing the positions of the interface and concentrations at the center of the taenite bands.

Previously, we found [3] that and impact onto a 100 km-radius differentiated planetesimal in the early Solar System can erode the insulating mantle and increase the cooling rate of the core by more than an order of magnitude. Specifically, we looked at a head-on impact 50 Myr after the planetesimal's formation. At this time, the mantle has nearly fully solidified but the core is still crystalizing. This increase in cooling rate would occur before the Widmanstäten pattern was fully developed (above temperatures of 450 C). As a result, we have carried out additional simulations, where the cooling rate of the core changes (increases) at some point to determine the effect on the resulting Ni concentration profile.

Figure 3 showcases one such example of this. In this case, the core was assumed to initially be cooling at 10 K/Myr, which is roughly the rate the core of a 100 km-radius planetesimal would cool [1]. During cooling, we increase the cooling rate to 500 K/Myr once the temperature dropped to 575 C, simulating the effects of an impact. Due to the more rapid cooling, Ni has less time to diffuse and for the taenite band to narrow. As a result, the disturbed profile has a wider band of taenite than the constant 10 K/Myr profile, though it is much narrower than the 500 K/Myr profile due to the diffusion that took during the slower cooling at high temperatures. The final half-width of the taenite band can be compared to other constant cooling rate cases, for which we found the closest match to be 23 K/Myr. However, while the band has nearly the same half-width, it does not have the central taenite Ni content is higher, closer to the 10 K/Myr case.

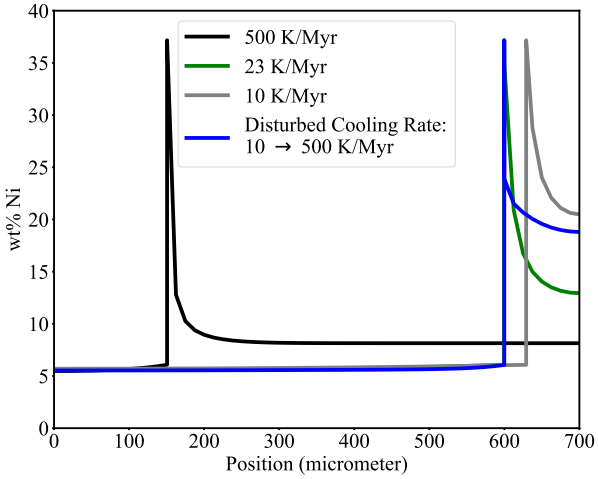

Figure 3: Ni concentration profiles looking at an impacted planetesimal. A 100 km radius body cools at 10 K/Myr (gray line), an impact occurs increasing the cooling rate to 500 K/Myr (black line), and the final impacted profile does not look like either two profiles (blue line). The closest match for the impact profile is that of a 23 K/Myr case (green line).

Discussion/Future Work: Given that impacts between planetesimals are expected to be common within the early Solar System [8], it is likely that some iron meteorite parent bodies should have had their cooling rates disturbed or altered during the development of the Widmanstäten pattern. Thus far, we have seen that a disturbed body may develop a Ni concentration profile with a taenite half-width that matches that of a constant cooling rate. This would lead to erroneous conclusions about the evolution of the parent body. However, the effect of the impact may be identified if the central Ni concentration differs substantially from that predicted by constant cooling rate calculations. We are continuing to explore the wide parameter space to quantify the effects that impacts would have on the properties of the iron meteorites, and will compare our predictions to what is found in the meteoritic data.

References: [1] Haack H. et al. (1990) JGR:SE 95, 5111 [2] Benedix G. K. et al. (2014) ToG 1, 267- 285 [3] Lyons et al. (2017) LPSC [4] Dauphas (2007) MaPS 42, 1597-1613 [5] Crank (1984) Clarendon Press, 425 p. [6] Hopfe and Goldstein (2001) MaPS 36, 135-154 [7] Jost (1952) Academic Press Inc., 558 p. [8] Davison T. M. et al. (2013) MaPS 48, 1894-1918